Arabian Journal of Chemistry (2023) **16**, 104765

King Saud University

Arabian Journal of Chemistry

www.ksu.edu.sa
www.sciencedirect.com

ORIGINAL ARTICLE

A novel NIR fluorescent probe for monitoring cysteine in mitochondria of living cells

Jianning Dong, Guowei Lu, Bin He, Yayi Tu *, Congbin Fan *

Jiangxi Key Laboratory of Organic Chemistry, College of Chemistry and Chemical Engineering, Jiangxi Science and Technology Normal University, Nanchang 330013, PR China

Received 30 October 2022; accepted 27 February 2023
Available online 5 March 2023

KEYWORDS

Cysteine;
Link-anthocyanin;
Acrylate;
NIR fluorescent probe;
Mitochondria-targeting;
Cell imaging

Abstract It has been demonstrated that the results caused by abnormal levels of Cysteine (Cys) are not negligible in biological processes. Furthermore, mitochondria are one of the most important organelles, which not only produce cellular energy, but also participate in signal transmission, growth, death, and other biological processes. Therefore, developing an efficient fluorescent probe targeting mitochondria to detect Cys in cells is useful for clinic pathological diagnosis. In this report, a near-infrared (NIR) fluorescent probe **LAA** based on link-anthocyanin as fluorophore and acrylate as identification groups has been prepared. Link-anthocyanin, as an NIR-emitting fluorophore, showed favorable water solubility and strong fluorescence intensity. Acrylate, as a recognition site, exhibited intense sensitivity and selectivity to Cys. In addition, **LAA** had a high tendency to localize to mitochondria due to the lipophilic positive ion in the link-anthocyanin. Under the excitation of 560 nm, the probe **LAA** could detect Cys with high selectivity and low detection limit (37 nM) at the emission of 670 nm, which belonged to the NIR range and was beneficial for biological application. Furthermore, **LAA** exhibited great biocompatibility and low cytotoxicity, which could monitor Cys in mitochondria of living cells in real-time.

1. Introduction

Cysteine (Cys), one of the significant biological thiols, plays a crucial role in biological systems (Kemp et al., 2008; Reddie and Carroll, 2008; Stuart A. Lipton et al., 2002). In biological systems, it has been confirmed that the abnormal intracellular concentration of Cys will lead to many diseases, such as growth retardation (Hammett, 1990; Mani et al., 2011), Alzheimer (McCaddon et al., 2003; Riederer et al., 2009), cardiovascular (Arduino A Mangoni et al., 2013; Yardim-Akaydin et al., 2003), Parkinson's diseases (Allain et al., 1995; Heafield et al., 1990) and so on. Therefore, developing a convenient and efficient technology for the detection of Cys is crucial for the diagnosis of related diseases. However, due to the similar chemical structure and properties of biothiols (Yin et al., 2017; Zhang et al., 2020), developing tools to differentiate Cys from homocysteine (Hcy) and glutathione (GSH) has become a research focus.

The emergence of the fluorescent probe method has quickly become a hot research topic (Dai et al., 2020; Liu et al., 2020; Wang et al., 2021; Yue et al., 2020; Zhang et al., 2022). But conventional flu-

* Corresponding authors.
E-mail addresses: tuyayi@126.com (Y. Tu), congbinfan@163.com (C. Fan).
Peer review under responsibility of King Saud University.

Production and hosting by Elsevier

https://doi.org/10.1016/j.arabjc.2023.104765
1878-5352

orescent probes have an apparent flaw that the emission wavelength is usually less than 650 nm. The fluorescence in this region is easily disturbed by cell self-fluorescence and light scattering to cause light damage in biological tissues, which severely limits its penetration depth and sensitivity to biological tissues and hinders its further application in living organisms (Kim et al., 2015; Li et al., 2019). Fortunately, the applications of near-infrared (NIR) fluorescent probes (emission wavelength of 650–900 nm) in deep tissue imaging have attracted more and more researchers' attention because of their low auto-fluorescence interference and slight photo-damage (Ren et al., 2020; She et al., 2021; Wang et al., 2021; Yang et al., 2021; Zhou et al., 2021; Zhang et al., 2020). More and more NIR fluorescent probes have been developed and reported in recent years.

Link-anthocyanin has been exploited as a sensor fluorophore in recent years. Anthocyanin, as good water-soluble flavonoids, was found in a wide range of biological applications, such as antioxidant, prevention of cardiovascular disease and antitumor (Borrás-Linares et al., 2015; Lin et al., 2017; Silva et al., 2016). As a modified fluorophore, link-anthocyanin not only maintained good water solubility, but also increased fluorescent properties, which made it become a hot sensor fluorophore that has attracted much attention from researchers (Chen et al., 2015; Li et al., 2021; Shang et al., 2017).

The detection and quantification of Cys in organelles are of great significance for prediction of diseases. Mitochondria, found in most eukaryotic cells, is one of the most important organelles. It is not only an energy field, but also participates in signal transmission, growth, death and other biological processes (Levine and Kroemer 2008; McBride et al., 2006; Xu et al., 2016). In addition, mitochondrial damage, including oxidative damage itself, leads to an imbalance between the production and removal of reactive oxygen species (ROS), resulting in net ROS production (Fang et al., 2022; Lin and Beal 2006;). However, biothiols with strong redox and nucleophilic properties are essential antioxidants that protect cells and tissues from endogenous ROS and free radical oxidation (A. Yu. Andreyev et al., 2005; Ren et al., 2018). Therefore, the detection of biothiols by fluorescence microscopy in mitochondria of living cells is conducive to clinicpathological analysis.

Based on the above-mentioned situations, a mitochondria-targeted NIR fluorescent probe **LAA** that specifically recognized Cys was exploited. The specific recognition and mitochondrial targeting were due to the introduction of acrylate as a recognition group in the link-anthocyanin fluorophore with lipophilic cation. **LAA** possessed excellent features as follows: a long emission wavelength at 670 nm; simple synthetic route; high selectivity and sensitivity to Cys with the detection limit of 3.7×10^{-8} M; low cytotoxicity; targeting mitochondria in living cells. The eminent optical properties and biocompatibility of **LAA** enabled it to be applied to detect Cys in living cells with mitochondria-targeting properties.

2. Experimental section

2.1. Materials and instruments

Some basic consumable materials used can be found in the supplementary material.

2.2. The process of preparation of LAA

The process of preparation of **LAA** is demonstrated in Scheme 1.

2.2.1. Synthesis of LA-OH

9-Formyl-8-hydroxyjulolidine (1.09 g, 5 mmol) was added to 30 mL glacial acetic acid contained 6-hydroxy-1-tetralone (0.81 g, 5 mmol), and then 2 mL perchloric acid (70%) was added to reflux for 2 h. After cooling to room temperature, the solution was eluted with 30 mL solution made of PE/EA (v/v, 1/1), then a black precipitate was formed which was filtered and washed with a small amount of ethanol for three times to produce **LA-OH** (Yield: 80%). The resulting filter cake is pure enough without further purification.

2.2.2. Synthesis of LAA

LA-OH (0.25 g, 0.5 mmol) and triethylamine (0.1 mL) were dissolved in dichloromethane (20 mL) at ice bath. Stirring for 5 min, dichloromethane solution (5 mL) containing acryloyl chloride (0.084 g, 1 mmol) was added drop by drop under the protection of argon. The reaction solution was stirred for 10 min, and then spin dry and further purified by column chromatography to obtain black solid **LAA** (yield: 90%). ^{1}H NMR (400 MHz, CD_2Cl_2) δ 8.46 – 8.04 (m, 2H), 7.43 (s, 1H), 7.40 – 7.18 (m, 2H), 6.64 (d, J = 17.1 Hz, 1H), 6.35 (dd, J = 17.4, 10.5 Hz, 1H), 6.10 (d, J = 10.4 Hz, 1H), 3.62 (d, J = 5.6 Hz, 4H), 3.35 – 2.91 (m, 8H), 2.36 – 2.01 (m, 4H) (Fig. S1). ^{13}C NMR (101 MHz, CD_2Cl_2) δ 163.8, 159.7, 154.7, 153.6, 153.1, 145.8, 142.9, 133.4, 129.7, 127.4, 127.4, 126.4, 124.4, 122.1, 121.4, 120.3, 119.9, 105.2, 51.5, 51.0, 27.7, 27.1, 25.0, 20.2, 19.5, 19.2. (Fig. S2). MS (ESI, m/z): Calcd for $[C_{26}H_{24}NO_3]^+$ 398.1751; found, 398.1744(Fig. S3).

2.3. Optical studies

The stock solution of **LAA** with the concentration of 1 mM was made in CH_3CN (HPLC grade). Cys and additional substances (Hcy, GSH, H_2S, Trp, Phe, Leu, Met, Tyr, Thr, Glu, Lys, Val, Asp, Ser, Gln, Pro, Ala, Gly, Asn, Ile, His, Arg) were prepared in deionized water. A 2 mL specific system, which was 1960 μL of phosphate-buffered saline (PBS) solution incorporating 50% CH_3CN (v/v, pH = 7.4) and 40 μL of the stock solution of **LAA**, was used as test system. After addition of Cys or other analytes, the obtained mixture was rocked to mix completely and stood for 15 min at room temperature, and then the UV–Vis absorption and fluorescent spectrum data were recorded. For fluorescent measurement, λ_{ex} = 560-nm, slit width: 5.0 nm/5.0 nm.

2.4. Cytotoxicity assay

Hela cells were seeded in 96-well plates and cultured in Dulbecco's Modified Eagle's medium (DMEM) containing 10% fetal bovine serum (FBS) for 24 h in the incubator. **LAA** was distributed into five concentrations (0, 10, 20, 40, 50 μM) and then added into 96-well plates for incubation of 24 h. After discarding the medium, a mixture of 10 μL 3-(4,5-dimethyl-2-thiazolyl)-2,5-diphenyl-2-H-tetrazolium bromide (MTT) (5 mg/mL) and 90 μL medium was added to each well, and the culture was continued for 4 h. At this time, blue-purple formazan was generated by succinate dehydrogenase in mitochondria of living cells, while dead cells could not reduce exogenous MTT to produce formazan crystal. The formazan dissolving solution (100 μL) was put into each well and incubated for another 4 h to dissolve the formed formazan. Cell viability was evaluated by the absorbance at 570 nm recorded by Multiskan FC assay (Thermo Scientific).

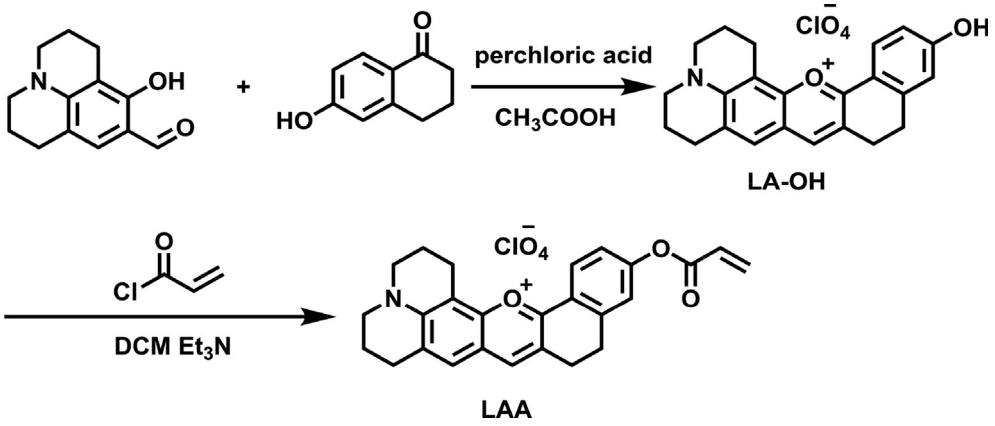

Scheme 1 Synthetic process of **LAA**.

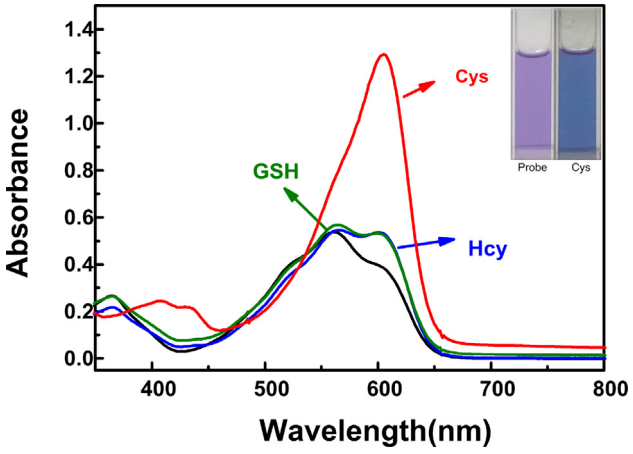

Fig. 1 UV–vis spectral changes of **LAA** (20 μM) in the presence of Hcy (100 μM), GSH (100 μM) and Cys (100 μM) respectively in PBS/CH_3CN (v/v = 1/1, pH = 7.4) solution.

2.5. Cell imaging

Hela cells, incubated in DMEM supplemented with 10% fetal bovine serum, 1% penicillin, and 1% streptomycin, were seeded in confocal dishes at 37 °C for 18 h in a CO_2 incubator (5% CO_2). Before using Olympus FV1000 confocal laser scanning microscope to take fluorescence imaging, all cells were washed with PBS three times. For imaging exogenous Cys, Hela cells were divided into four groups. The first group was the blank group containing Hela cells only as background control. The second group was the test control group that **LAA** (20 μM) was incubated in Hela cells for 30 min before imaging. In the third group, Hela cells were pretreated with N-ethylmaleimide (NEM, 500 μM) for 30 min, then washed with PBS three times and **LAA** (20 μM) was added to the culture for another 30 min. For the fourth group, NEM (500 μM) was incubated with Hela cells for 30 min, then washed with PBS three times and **LAA** (20 μM) was added into the cell-culture dish to incubate for another 30 min. After the disposal of the medium, Hela cells were rinsed with PBS buffer three times

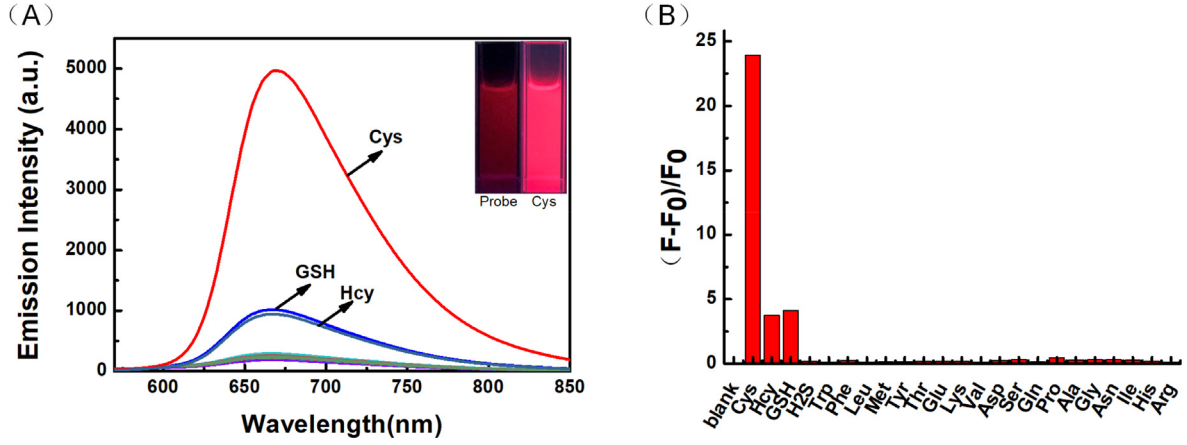

Fig. 2 (A) Fluorescent selectivity curve (B) Emission intensity fold plot of probe **LAA** (20 μM) toward various analytes (100 μM) in PBS/CH_3CN (v/v = 1/1, pH = 7.4) solution (λ_{ex} = 560 nm, slit: 5.0/5.0 nm).

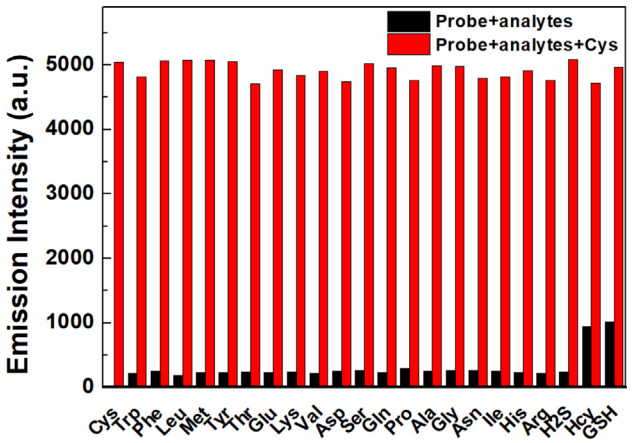

Fig. 3 Fluorescent responses of **LAA** (20 μM) toward Cys (100 μM) in the presence of interfering analytes (100 μM) in PBS/CH_3CN (v/v = 1/1, pH = 7.4) solution (λ_{ex} = 560 nm, slit: 5.0/5.0 nm).

and handled with Cys (50 μM) for an additional 30 min before imaging. For the co-localization performance study, commercial Mito-Tracker Green (Beyotime Biotechnology) was added into Hela cells in the fourth group and incubated for 30 min. Co-localization was analyzed using ImageJ software.

3. Results and discussion

3.1. UV spectrum response of LAA to Cys

In order to study the selective recognition of Cys by **LAA**, we studied the UV–Vis absorption spectrum characteristics of the probe in response to Cys, Hcy and GSH in PBS/CH_3CN (v/v = 1/1, pH = 7.4). Cys (100 μM) was added to the test solution, the maximum absorption peak increased obviously and the adsorption effect was redshift to 600 nm, while the addition of Hcy (100 μM) and GSH (100 μM) caused minor changes (Fig. 1). Meanwhile, the color of the solution changed from purple to light blue (insert). These results demonstrated that **LAA** can recognize Cys specifically over Hcy and GSH.

3.2. The selectivity of LAA to Cys

A good selective response is also necessary for the satisfactory detection of a target substance in a complex biological sample. To investigate the selectivity of **LAA** to Cys, various relevant analytes (100 μM) were added respectively into 2 mL specific system and the fluorescent spectra were recorded. As displayed in Fig. 2A, after adding Cys, an emission peak emerged in 670 nm and increased sharply, while Hcy, GSH and other analytes caused negligible effects. At the meantime, the fluorescent color of the test system changed from a very weak dark

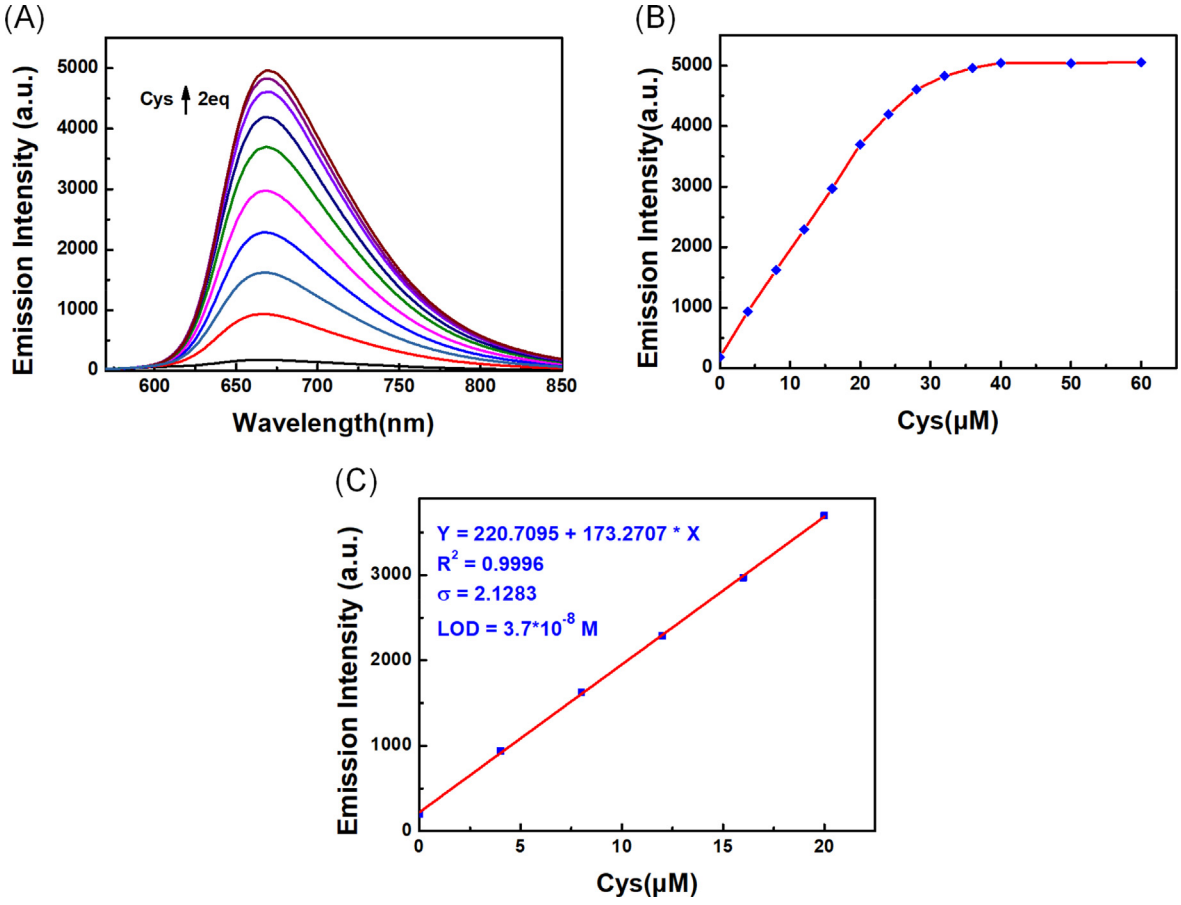

Fig. 4 (A) Fluorescent titration (B) Variation curve of emission intensity value (C) The linear relationship of **LAA** (20 μM) response to Cys in PBS/CH_3CN (v/v = 1/1, pH = 7.4) solution (λex = 560 nm, slit: 5.0/5.0 nm).

fluorescence to a very strong bright red fluorescence (insert). Moreover, as displayed in Fig. 2B, the fluorescent intensity of the test solution after adding Cys increased 24-fold, while Hcy and GSH only caused 3.7-fold and 4.1-fold increasement, respectively. These results demonstrated that **LAA** could recognize Cys selectively.

In order to investigate the effect of other analytes on the detection of Cys by **LAA**, competitive experiments were conducted to test the anti-interference ability of the probe. As shown in Fig. 3, after adding 100 μM Cys to the system containing 20 μM **LAA** and 100 μM other analytes, the fluorescent intensity at 670 nm was not affected in the presence of various analytes, demonstrating a good anti-interference ability of LAA in the detection of cysteine.

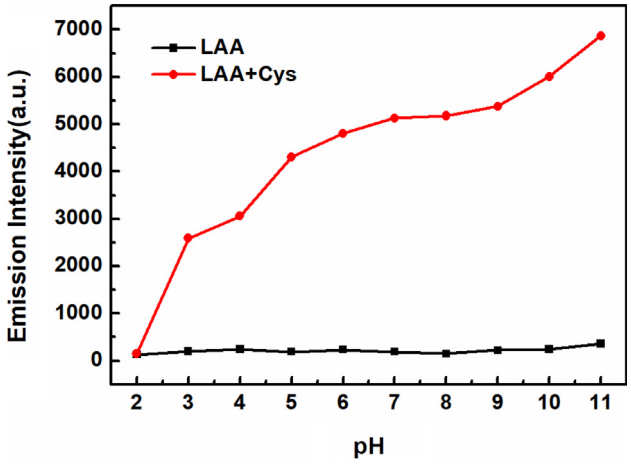

Fig. 5 The effect of different pH value on the fluorescent intensity of **LAA** (20 μM) with or without Cys (100 μM).

3.3. The sensitivity of LAA to Cys

For the purpose of examining the sensitivity of **LAA** to Cys, we investigated the fluorescent intensity of the probe in response to different concentrations of Cys. As shown in Fig. 4A and Fig. 4B, a range of fluorescent spectra of 20 μM probe solutions containing different concentrations of Cys were recorded. With the increase of Cys concentration, the emission intensity at 670 nm gradually increased and reached a stable level at 2 equal quantities. As shown in Fig. 4C, in the range of 0 to 20 μM, the emission intensity was linearly correlated with the concentrations of Cys, and the limit of detection (LOD) of Cys was as low as 3.7×10^{-8} M. These results indicated that the probe **LAA** had high sensitivity to Cys.

3.4. Effect of pH value

In order to investigate the effect of pH on the detection of Cys by **LAA**, fluorescent intensity at different pH values were measured. As shown in Fig. 5, **LAA** exhibited weak and steady fluorescent emission in the pH range of 2 to 11 under the excitation wavelength at 560 nm. After adding 100 μM Cys, an obvious fluorescence enhancement was observed in the pH range of 3 to 11. The fluorescent intensity was stable over a wide pH range from 6 to 9 in the detection of Cys by **LAA**. At the condition of pH > 9, a significant enhancement of fluorescent intensity appeared. The hydroxyl group on **LA-OH** generated by the reaction of **LAA** and Cys easily lost protons to produce oxyanions under alkaline condition, which enhanced the fluorescent intensity by a stronger ICT effect. When the pH was less than 6, the effect of protonation made the fluorescent intensity decrease. The results showed that the recognition of Cys by **LAA** was not affected by pH values in physical conditions, indicating the possible use of the probe in biological environment.

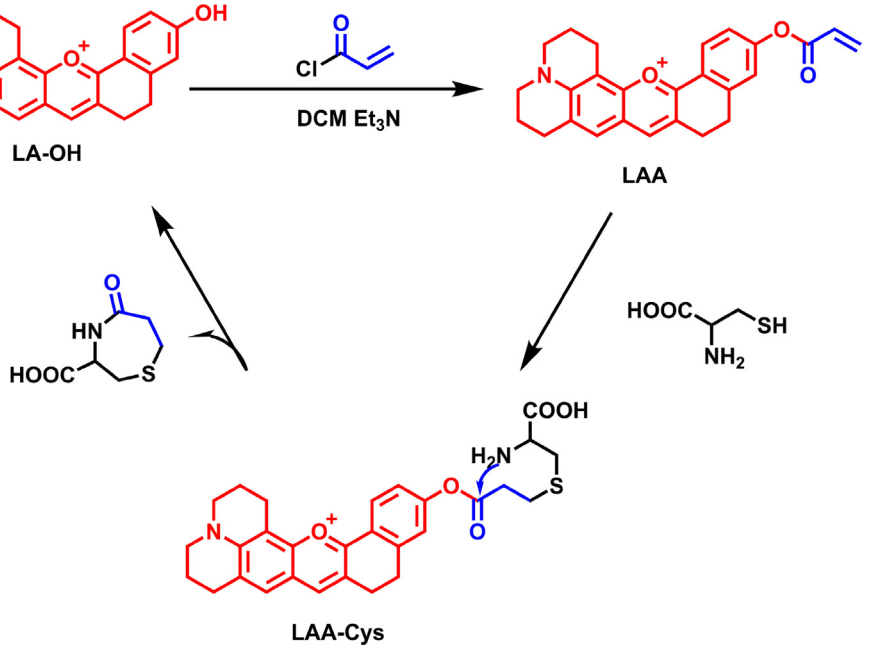

Scheme 2 The proposed mechanism of **LAA** for the detection of Cys.

3.5. Sensing mechanism

A NIR fluorescent probe **LAA** based on link-anthocyanin for specific detection of Cys has been prepared. The proposed mechanism for recognition of Cys is shown in Scheme 2. Cys could break the acryloyl to generate intermediate **LAA-Cys** by addition with double bonds, and then underwent intramolecular cyclization to remove a seven-membered ring compound and release the fluorophore **LA-OH**, which exhibited strong fluorescence. The proposed sensing mechanism was proved by MS detection of the mixed solution of **LAA** and Cys. The mass spectrum presented a dominant peak of m/z at 344.1642, which was almost equal to **LA-OH** ($M + H^+ = 344.1645$) (Fig. S4).

3.6. Test strip experiment

In order to explore the application of **LAA** *in vitro*, the test strip experiment was conducted. We first soaked the test strips in **LAA** solution (1 mM) for 10 s, and then placed them on glasses and dried in the air. The test strips containing **LAA** were immersed in aqueous solution of different analytes (1 mM). After drying, photographs were taken in natural light and under 365 nm ultraviolet lamps. As shown in Fig. 6, only the test strip immersed in Cys aqueous solutions exhibited significant color change, which showed strong red fluorescence. Test strips immersed in Hcy and GSH showed purple fluorescence, and others exhibited blue fluorescence. The result demonstrated that **LAA** could simply and quickly recognize Cys *in vitro*.

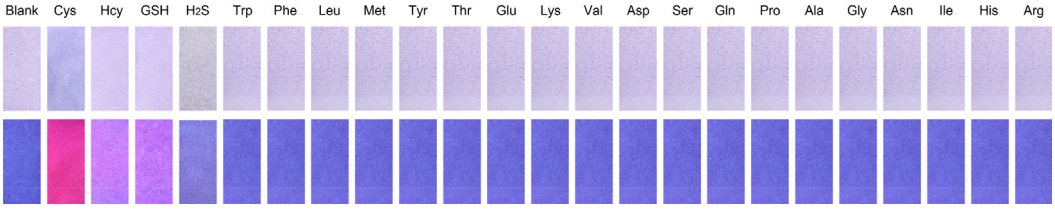

Fig. 6 Color changes of **LAA** test strips with different analytes photographed under natural light (top line) and 365 nm UV lamp (bottom line).

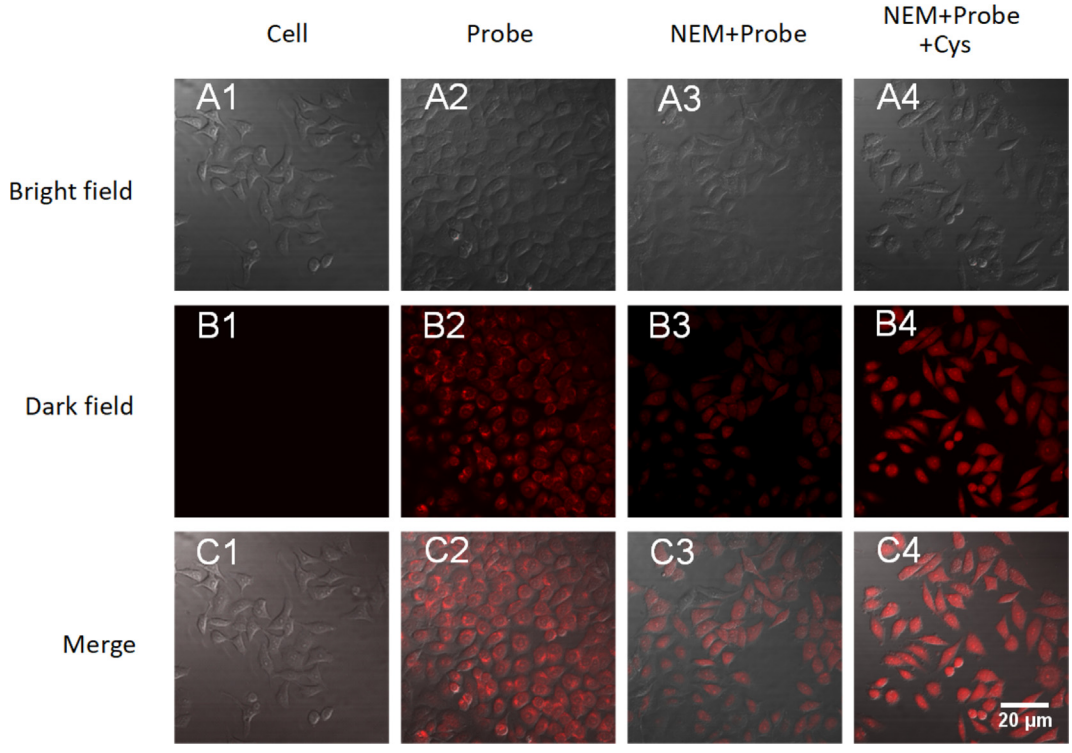

Fig. 7 Confocal fluorescence images of **LAA** in Hela cells. (A1-C1) Hela cells only. (A2-C2) Hela cells incubated with probe **LAA** (20 μM). (A3-C3) Hela cells incubated with NEM (500 μM) and **LAA** (20 μM). (A4-C4) Hela cells incubated with NEM (500 μM), **LAA** (20 μM) and Cys (50 μM). Scale Bar: 20 μm.

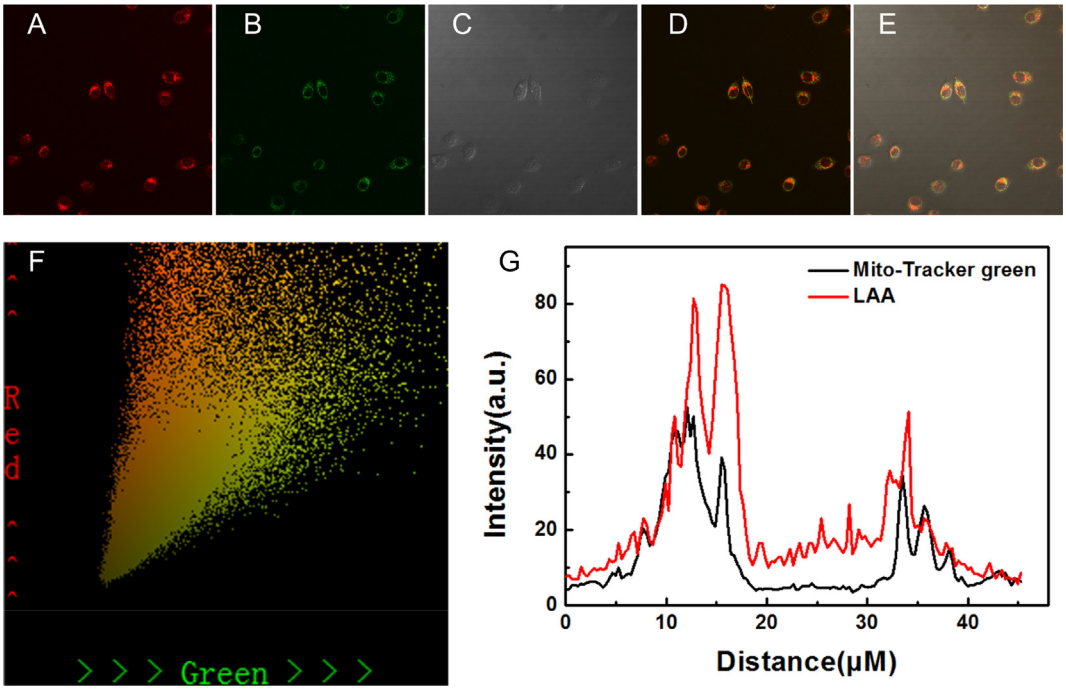

Fig. 8 Co-localization of **LAA** with mitochondria in Hela cells. (A) Red channel; (B) Green channel; (C) Bright field; (D) Merged image of (A) and (B); (E) Merged image of (A), (B) and (C); (F) The correlation of **LAA** and Mito-Tracker Green; (G) Intensity profile of regions of interest across HeLa cells.

3.7. Cell imaging

For analyzing the detection and imaging application of **LAA** to Cys in living cells, the viability of Hela cells under different **LAA** concentrations (0, 10, 20, 40, 50 μM) was determined by MTT assay. As shown in Fig. S5, even at the concentration of 50 μM **LAA**, the cell viability was still greater than 80%, which indicated that **LAA** had good biocompatibility.

To explore the biological application of **LAA** to detect Cys in living cells, cell imaging experiment was conducted. Hela cells were used as a background control (Fig. 7A1-C1). Hela cells incubated with **LAA** (20 μM) for 30 min exhibited obvious red fluorescence, which suggested that **LAA** could recognize endogenous Cys (Fig. 7A2-C2). However, when pretreated with NEM (500 μM) for 30 min and then incubated with **LAA** for another 30 min, Hela cells showed very weak fluorescence (Fig. 7A3-C3). For further study of the function of **LAA** to detect Cys, Hela cells were pretreated with NEM and **LAA** sequentially for 30 min and then incubated with Cys (50 μM) for an additional 30 min, which showed remarkable red fluorescence (Fig. 7A4-C4). These results confirmed that **LAA** could be used to detect Cys in living Cells.

3.8. Studies on the performance of localizing mitochondria

Generally speaking, lipophilic positive ion has a high tendency to localize in the mitochondria due to strong negative membrane potential in the mitochondrial matrix. Hence, the mitochondrial localization ability of **LAA** was evaluated by co-localization experiments. A commercial mitochondrial marker, Mito-Tracker green, was used to test whether **LAA** could localize to mitochondria in living cells. As shown in Fig. 8, the red channel fluorescence of **LAA** overlapped well with the green channel fluorescence of Mito-Tracker green. According to the correlation of **LAA** and Mito-Tracker Green (Fig. 8F), the Pearson's correlation was calculated to be 0.80, which indicated that **LAA** had a good accumulation capacity in mitochondria.

4. Conclusions

In summary, we have designed a novel mitochondria-targetable NIR fluorescent probe **LAA** for monitoring cysteine in living cells. **LAA** exhibited high sensitivity and selectivity toward Cys based on the acrylate identification unit. In addition, as a NIR fluorescent probe, **LAA** exhibited great biocompatible and low cytotoxicity for real-time monitoring of Cys in mitochondrial in living cells. The probe could also be used as test strips for the detection of Cys. Due to the advantages of low auto-fluorescence and slight photodamage, the NIR probe **LAA** could be used as a potential detection tool for Cys monitoring in mitochondria.

Acknowledgment

This work was supported by the National Natural Science Foundation of China (21861017, 32260017), the Project of the Science Funds of Jiangxi Education Office (GJJ211124) and Jiangxi Provincial Natural Science Foundation (20202BAB215003, 20212BAB215005).

Appendix A. Supplementary data

Supplementary data to this article can be found online at https://doi.org/10.1016/j.arabjc.2023.104765.

References

Allain, P., Le Bouil, A., Cordillet, E., et al, 1995. Sulfate and cysteine levels in the plasma of patients with Parkinson's disease. Neurotoxicology 16, 527–529.

Andreyev, A.Y., Kushnareva, Y.E., Starkov, A.A., 2005. Mitochondrial Metabolism of Reactive Oxygen Species. Biochemistry (Moscow). 70, 200–214.

Borrás-Linares, I., Fernández-Arroyo, S., Arráez-Roman, D., et al, 2015. Characterization of phenolic compounds, anthocyanidin, antioxidant and antimicrobial activity of 25 varieties of Mexican Roselle (Hibiscus sabdariffa). Ind. Crops Prod. 69, 385–394.

Chen, H., Lin, W., Jiang, W., et al, 2015. Locked-flavylium fluorescent dyes with tunable emission wavelengths based on intramolecular charge transfer for multi-color ratiometric fluorescence imaging. Chem. Commun. (Camb) 51, 6968–6971.

Dai, J., Ma, C., Zhang, P., et al, 2020. Recent progress in the development of fluorescent probes for detection of biothiols. Dyes Pigm. 177, 108321.

Fang, S., Wang, L., Mei, Y., et al, 2022. A ratiometric fluorescent probe for sensing hypochlorite in physiological saline, bovine serum albumin and fetal bovine/calf serum. Spectrochim. Acta. A Mol. Biomol. Spectrosc. 269, 120738.

Hammett, F.S., 1990. Growth retardation by the partially oxidized sulfhydryl of cysteine. Science. 77, 190–191.

Heafield, M.T., Fearn, S., Steventon, G.B., et al, 1990. Plasma cysteine and sulphate levels in patients with motor neurone, Parkinson's and Alzheimer's disease. Neurosci. Lett. 110, 216–220.

Kemp, M., Go, Y.M., Jones, D.P., 2008. Nonequilibrium thermodynamics of thiol/disulfide redox systems: a perspective on redox systems biology. Free Radic. Biol. Med. 44, 921–937.

Kim, D., Moon, H., Baik, S.H., et al, 2015. Two-Photon Absorbing Dyes with Minimal Autofluorescence in Tissue Imaging: Application to in Vivo Imaging of Amyloid-beta Plaques with a Negligible Background Signal. J. Am. Chem. Soc. 137, 6781–6789.

Levine, B., Kroemer, G., 2008. Autophagy in the pathogenesis of disease. Cell. 132, 27–42.

Li, H., Chen, R., Jiang, Y., et al, 2021. A two-photon fluorescent probe based on link-anthocyanin for detecting cysteine in nucleoli and lysosomes. Sens. Actuators B: Chem. 329, 129159.

Li, M., Zheng, K., Chen, H., et al, 2019. A novel 2,5-bis(benzo[d]thiazol-2-yl)phenol scaffold-based ratiometric fluorescent probe for sensing cysteine in aqueous solution and serum. Spectrochim. Acta. A Mol. Biomol. Spectrosc. 217, 1–7.

Lin, M.T., Beal, M.F., 2006. Mitochondrial dysfunction and oxidative stress in neurodegenerative diseases. Nature. 443, 787–795.

Lin, B.W., Gong, C.C., Song, H.F., et al, 2017. Effects of anthocyanins on the prevention and treatment of cancer. Br. J. Pharmacol. 174, 1226–1243.

Lipton, S.A., Choi, Y.-B., Takahashi, H., et al, 2002. Cysteine regulation of protein function – as exemplified by NMDA-receptor modulation. Trends neurosci. 25, 474–480.

Liu, X., Li, N., Li, M., et al, 2020. Recent progress in fluorescent probes for detection of carbonyl species: Formaldehyde, carbon monoxide and phosgene. Coord. Chem. Rev. 404, 213109.

Mangoni, A.A., Zinellu, A., Carru, C., et al, 2013. Serum thiols and cardiovascular risk scores: a combined assessment of transsulfuration pathway components and substrate/product ratios. J. Transl. Med. 11, 99.

Mani, S., Yang, G., Wang, R., 2011. A critical life-supporting role for cystathionine gamma-lyase in the absence of dietary cysteine supply. Free Radic. Biol. Med. 50, 1280–1287.

McBride, H.M., Neuspiel, M., Wasiak, S., 2006. Mitochondria: more than just a powerhouse. Curr. Biol. 16, 551–560.

McCaddon, A., Hudson, P., Hill, D., et al, 2003. Alzheimer's disease and total plasma aminothiols. Biol. Psychiatry. 53, 254–260.

Reddie, K.G., Carroll, K.S., 2008. Expanding the functional diversity of proteins through cysteine oxidation. Curr. Opin. Chem. Biol. 12, 746–754.

Ren, H.X., Huo, F.J., Zhang, Y.B., et al, 2020. An NIR ESIPT-based fluorescent probe with large stokes shift for specific detection of Cys and its bioimaging in cells and mice. Sens. Actuators B: Chem. 319, 128248.

Ren, T.-B., Zhang, Q.-L., Su, D., et al, 2018. Detection of analytes in mitochondria without interference from other sites based on an innovative ratiometric fluorophore. Chem. Sci. 9, 5461–5466.

Riederer, I.M., Schiffrin, M., Kovari, E., et al, 2009. Ubiquitination and cysteine nitrosylation during aging and Alzheimer's disease. Brain Res. Bull. 80, 233–241.

Shang, H., Chen, H., Tang, Y., et al, 2017. Development of a two-photon fluorescent turn-on probe with far-red emission for thiophenols and its bioimaging application in living tissues. Biosens. Bioelectron. 95, 81–86.

She, Z.-P., Wang, W.-X., Mao, G.-J., et al, 2021. A near-infrared fluorescent probe for accurately diagnosing cancer by sequential detection of cysteine and H+. Chem. Commun. 57, 4811–4814.

Silva, V.O., Freitas, A.A., Maçanita, A.L., et al, 2016. Chemistry and photochemistry of natural plant pigments: the anthocyanins. J. Phys. Org. Chem. 29, 594–599.

Wang, K., Wang, W., Guo, M.-Y., et al, 2021a. Design and synthesis of a novel "turn-on" long range measuring fluorescent probe for monitoring endogenous cysteine in living cells and Caenorhabditis elegans. Anal. Chim. Acta. 1152, 338243.

Wang, Y., Yu, H., Zhang, Y., et al, 2021b. Development and application of several fluorescent probes in near infrared region. Dyes Pigm. 190, 109284.

Xu, W., Zeng, Z., Jiang, J.H., et al, 2016. Discerning the Chemistry in Individual Organelles with Small-Molecule Fluorescent Probes. Angew. Chem. Int. Ed. 55, 13658–13699.

Yang, Y., Feng, Y., Li, H., et al, 2021. Hydro-soluble NIR fluorescent probe with multiple sites and multiple excitations for distinguishing visualization of endogenous Cys/Hcy, and GSH. Sens. Actuators B: Chem. 333, 129189.

Yardim-Akaydin, S., Ozkan, Y., Ozkan, E., et al, 2003. The role of plasma thiol compounds and antioxidant vitamins in patients with cardiovascular diseases. Clin. Chim. Acta. 338, 99–105.

Yin, C.X., Xiong, K.M., Huo, F.J., et al, 2017. Fluorescent Probes with Multiple Binding Sites for the Discrimination of Cys, Hcy, and GSH. Angew. Chem. Int. Ed. Engl. 56, 13188–13198.

Yue, Y., Huo, F., Yin, C., 2020. The chronological evolution of small organic molecular fluorescent probes for thiols. Chem. Sci. 12, 1220–1226.

Zhang, S., Liao, W., Wang, X., et al, 2022. An indanone-based fluorescent probe for detection and imaging of Cys/Hcy in living cells. Spectrochim. Acta. A Mol. Biomol. Spectrosc. 279, 121364.

Zhang, R., Yong, J., Yuan, J., et al, 2020a. Recent advances in the development of responsive probes for selective detection of cysteine. Coord. Chem. Rev. 408, 213182.

Zhang, Y., Zhang, Y., Yue, Y., et al, 2020b. Based on morpholine as luminescence mechanism regulation and organelle targeting dual function Cys NIR specific biological imaging probe. Sens. Actuators B: Chem. 320, 128348.

Zhou, K., Yang, Y., Zhou, T., et al, 2021. Design strategy of multifunctional and high efficient hydrogen sulfide NIR fluorescent probe and its application in vivo. Dyes Pigm. 185, 108901.